Letters

Metal/CdTe/CdS/Cd$_{1-x}$Zn$_x$S/TCO/glass: A new CdTe thin film solar cell structure

Isaiah O. Oladeji[a], Lee Chow[a,*], Christos S. Ferekides[b],
Vijay Viswanathan[b], Zhiyong Zhao[b]

[a]*Department of Physics, University of Central Florida, Orlando, FL 32816, USA*
[b]*Department of Electrical Engineering, University of South Florida, Tampa, FL 33620, USA*

Abstract

The potential of CdTe/CdS/Cd$_{1-x}$Zn$_x$S structure as an alternative to CdTe/CdS structure in photovoltaic application has been demonstrated. The unoptimized solar cell structure grown on transparent conducting oxide coated soda lime glass of 3 mm thickness with no antireflection coating yielded a 10% efficiency. This efficiency is the highest ever recorded in any Cd$_{1-x}$Zn$_x$S film containing CdTe solar cells. © 2000 Elsevier Science B.V. All rights reserved.

Keywords: CdTe; Solar cell; CdZnS

1. Introduction

The average solar radiation [1] reaching the earth surface, AM1.5, is very rich in photons with energies ranging from about 1.4 eV–3 eV. In traditional CdTe solar cells CdS is popularly used as a window material and as an n-type heterojunction partner to p-CdTe. Since the bandgaps of CdTe and CdS are 1.5 and 2.4 eV, respectively, it means that only photons with energies within this range reach CdTe layer where they contribute to the cell's photocurrent. The absorption coefficients of II–VI compounds in the spectrum window are high [2], about 10^4–10^5 cm^{-1}. Thus, the carrier generation by higher energy photons in the n-CdS layer takes place at the surface far away

---

* Corresponding author. Tel.: 001-4078-232-325; fax: 001-4078-235-112.
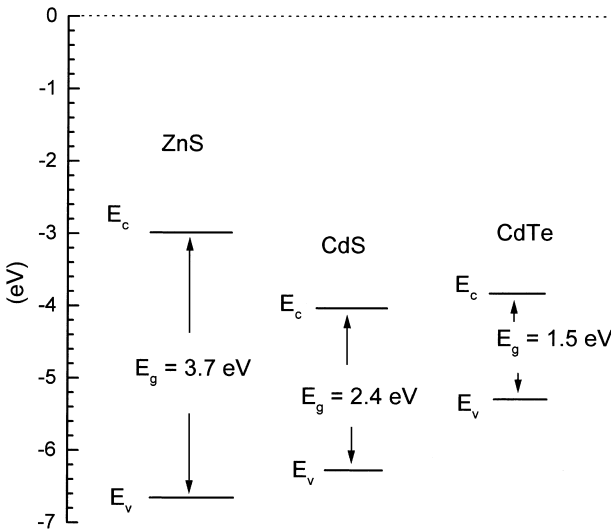*E-mail address:* le@physics.ucf.edu (L. Chow)

Fig. 1. Band edge energies of ZnS, CdS, and CdTe compounds [6]. Where E_g is the band gap, E_c conduction band edge, and E_v valence band edge.

from the depletion region where the generated carriers can be collected. As a result, these carriers are often lost to surface recombination current. This current increases the dark current and consequently reduces the useful current delivered by the cell to a load. In these CdS/CdTe cells, reducing the thickness of CdS layer [3] to less than 1000 Å is routinely done to reduce the absorption and minimize the surface recombination current. At this thickness they appear to be low yield due to increase in the shunting probability. Below 700 Å, there is a general degradation [3] in the cell performance owing to considerable decrease in shunt resistance. It should have, therefore, been more appropriate to use a thick layer of ZnS film with 3.7 eV bandgap as a window, but there are several drawbacks associated with this idea. First, ZnS is highly resistive and hard to dope [4] and could significantly increase the cell's series resistance. Second, the lattice mismatch between ZnS and CdTe is about 16%, making it a poorer heterojunction partner to CdTe compare to CdS. Depositing CdTe directly on a thick $Cd_{1-x}Zn_xS$ film will not help either, because detrimental property, especially lattice constant [5], of this film lies between those of CdS and ZnS. The arguments above then make $Cd_{1-x}Zn_xS$/CdS structure a suitable window structure that can maintain the traditional CdS/CdTe contact and improve the short wavelength spectral response of the cell at the same time, without compromising the transport properties, the series and the shunt resistances of the cell.

Let us look at the feasibility of CdTe/CdS/$Cd_{1-x}Zn_xS$ structure for solar cell application from the band structure standpoint. According to Lehmann [6] the relative position of conduction and valence band edges of ZnS, CdS, and CdTe are as shown in Fig. 1. Based on the relative positions of the band edges of these materials, an efficient cell is only possible with ZnS heavily n-type doped, CdS lightly doped, and
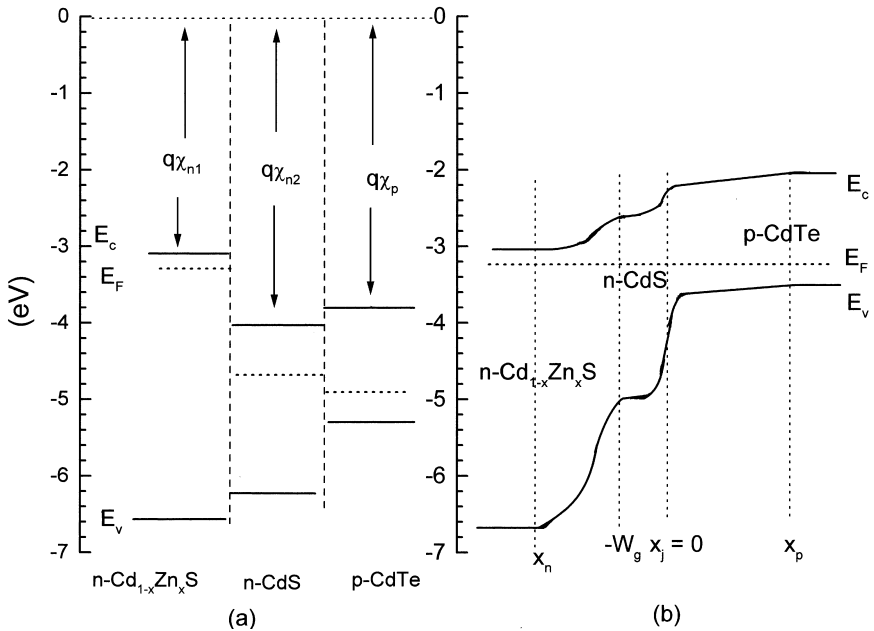
Fig. 2. Ideal band diagrams of $Cd_{1-x}Zn_xS/CdS/CdTe$ system (a) before and (b) after junction formation. Where $q\chi_n$ is the electron affinity in the n-type semiconductor and $q\chi_p$ that in the p-type semiconductor, E_F the Fermi level, x_j the CdS/CdTe metallurgical junction, W_g original CdS layer thickness, x_n and x_p are depletion layer edges in the n and p-type regions, respectively.

a normal p-type doped CdTe films. But the difficulty in doping ZnS makes $Cd_{1-x}Zn_xS$ a suitable alternative. As a result the latter shall be used as the doped form of ZnS. The conduction and valence band edges of this material lie between [5] those of ZnS and CdS depending on the Zn or Cd content. After doping, the band structure of the films before and after the junction formation is shown in Fig. 2(a) and (b), respectively. In Fig. 2(b), the high electron affinity (χ_n) of CdS compared to that of CdTe (χ_p) helps eliminate the energy spike at the CdS/CdTe junction. At the $Cd_{1-x}Zn_xS/CdS$ interface we also note that there is no energy spike. This is because these materials are highly soluble [6] into each other, and the graded junctions between them do exist in which band edges change over certain distance with a finite slope corresponding to electric field strength. For a thin CdS film, the slope covers the whole of this intermediate layer. This, coupled with the high conductivity of doped $Cd_{1-x}Zn_xS$ layer ensure [7] that the depletion region extends through out the original thickness, W_g, of CdS layer and up to x_p in the CdTe layer. Under AM1.5 illumination, if $Cd_{1-x}Zn_xS$ is transparent to this spectrum, the carriers generated by the higher energies photons down to 2.4 eV in the CdS layer, now well removed from the cell surface, are no longer lost to surface recombination. Instead, they are separated and collected by the assistance of the field present in this region. The consequence therefore is a strong spectral response of the solar cell in almost all

AM1.5 spectrum resulting in higher efficiency CdTe solar cell. The objective of this study is to demonstrate that the traditional 'Metal/CdTe/CdS/TCO/glass' structure of CdTe solar cells can be changed to 'Metal/CdTe/CdS/Cd$_{1-x}$Zn$_x$S/TCO/glass' which has the potential of attaining the highest efficiency ever recorded in CdTe solar cells.

2. Experimental

CBD and CSS were used to grow the window and the absorber layers of Cd$_{1-x}$Zn$_x$S/CdS/CdTe solar cell structures, respectively. The Cd$_{1-x}$Zn$_x$S layer was formed from the processed CBD grown ZnS/CdS multilayer. The CBD growth of CdS thin films was carried out in a 80°C, 140 ml stirred solution consisting of 18.4 MΩ deionized water, 0.05 g cadmium acetate dihydrate (Cd(CH$_3$COO)$_2$ · H$_2$O), 0.1 g ammonium acetate (NH$_4$CH$_3$COO), 6.5 ml ammonium hydroxide (NH$_4$OH) of normality 14.3, and 0.03 g thiourea (SC(NH$_2$)$_2$). The CBD growth of ZnS thin films, on the other hand, was carried out in a similar bath at 50°C where the reagents are 0.4 g zinc sulfate heptahydrate (ZnSO$_4$ · 7H$_2$O), 0.4 g ammonium sulfate (NH$_4$)$_2$SO$_4$), 0.11 g thiourea (SC(NH$_2$)$_2$), 6 ml ammonium hydroxide (NH$_4$OH) of normality 14.3, 10 ml of 100% hydrazine monohydrate (N$_2$H$_4$ · H$_2$O), and 0.5 g of nitrilotriacetic acid dissolved in 1.45 ml KOH solution. For the CdTe films deposition closed space sublimation (CSS) reactor was used. Here, the 99.999% pulverized CdTe powder source at 650°C in 15–30 torr He/O$_2$ mixture ambient was sublimated onto a substrate at 600°C which was 0.2 cm away from the source.

Our primary substrate was a cleaned Libbey Owens Ford TEC 8 transparent conducting oxide coated soda lime glass of 3 mm thickness. The superstrate for the deposition of CdTe were of two types:

(1) In the first type, a 0.07 μm thick ZnS film was first deposited on TCO/glass substrate. This was then dipped in 1% CdCl$_2$ methanol solution for about 30 s to improve the conductivity, then dried with an infrared lamp, and then rinsed in the deionized water. This was followed by an additional deposition of 0.05 μm CdS thin film to complete the superstrate fabrication. The solar cells fabricated from these substrates are called type 1.

(2) In the second type, a 0.03 μm thick CdS film sandwiched between two 0.04 μm thick ZnS films were first deposited by CBD on TCO/glass substrate. The glass multilayers substrate was then given the usual CdCl$_2$ treatment described above. The sample was then annealed in CdCl$_2$/Ar ambient at 400°C for 15 min. The substrate fabrication was completed by the deposition of an additional 0.035 μm thick CdS film. The solar cells fabricated from these ones are called type 2.

We need to note that the in-situ diffusion of Cd into ZnS layer in the CdS growth bath is quite significant. This together with the low temperature annealing ensured the formation of Cd$_{1-x}$Zn$_x$S/CdS layer as reported elsewhere [8].

Prior to the deposition of CdTe in each case the CdS/Cd$_{1-x}$Zn$_x$S/TCO/glass structure was further annealed in situ in the CSS reactor chamber in H$_2$ ambient for

about 15 min. For the purpose of comparison a CdS/CdTe structure was also fabricated.

In all cases after CdTe deposition, the structure was treated with $CdCl_2$, annealed in He/O_2 ambient at $400°C$, and etched in 0.5% Br_2 methanol solution to form Te rich surface. The structures were then masked; Cu doped graphite contact applied and processed, and the cells isolated. Indium was soldered on TCO around each device to improve current collection.

To determine the extent of Zn diffusion SIMS analysis were performed on types 1 and 2 cells from which the contacts were stripped. SIMS data were taken using a CAMECA IMS-3f with O_2^+ primary beam and detection of secondary positive ions. The impact energy was 5.5 keV. Typical sputtering conditions were 150 nA O_2^+ into a $200 \, \mu m \times 200 \, \mu m$ crater. Ions were detected from $60 \, \mu m$ diameter region at the center of the crater.

Illuminated $I–V$ measurements were performed on the cells using xenon-arc lamp simulator with NREL-confirmed devices. The $J–V$ curves were used to extract V_{oc}, series, and shunt resistance. External quantum efficiency (QE) measurements were performed using zero-light bias with total intergrated current set to measure J_{sc} of each device.

3. Results and discussions

The solar cell data extracted from the illuminated $J–V$ characteristics of Fig. 3 are summarized in Table 1. From Table 1 and Fig. 3, we observe that the J_{sc} of the type 1 cell is the highest and that of CdS/CdTe is the least. The explanation of these observations is straightforward by taking a closer look at the spectral response curves, Fig. 4, of the cells. In the following order CdS/CdTe, type 1, and type 2 $Cd_{1-x}Zn_{1-x}S$/CdS/CdTe solar cells have 80% or slightly higher QE in the 600–850 nm, 525–850 nm, and 510–850 nm wavelength regions. Below these regions, at 500 nm, say, the QE is about 62% for CdS/CdTe cell, 65% for type 1 cell, and 75% for type 2 cell; and at 400 nm, the QE are 38%, 40%, and 38% in that same order. We note that cells with $Cd_{1-x}Zn_xS$ layer (Types 1 and 2 cells) generally have better short wavelength response, as expected, and may explain why they have higher J_{sc}. However, for these same type of cells, between 550 and 850 nm the QE of type 2 cell is slightly lower than that of type 1, but from 450 to 550 nm the QE of type 2 cell is higher than that of type 1. This slight response reversal may explain why the J_{sc} of types 1 and 2 cells differ by only 0.1 mA/cm^2 in favor of type 1. The reduced J_{sc} and QE between 550 and 850 nm of type 2 cell could be as a result of some recombination at the interface due possibly to stress induced defects. The low V_{oc} of type 2 cell, and type 1 cell for that matter, seems to confirm our speculation, since these defects are reported to have stronger impact [9,10] on this parameter.

To find a possible source of these interface defects that reduce the V_{oc} of type 1 and type 2 cells, we consider the SIMS analysis, Fig. 5, of these cells. Zn seems to have diffused through to the CdS/CdTe interface and more into CdTe layer in the type 2 cell than in the type 1 cell. It is known that lattice mismatch of $Cd_{1-x}Zn_xS$/CdTe is
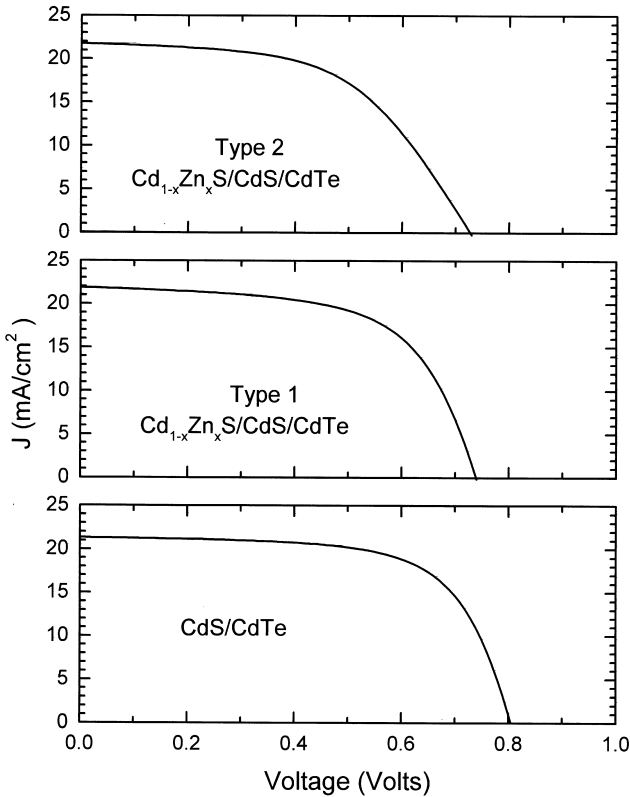
Fig. 3. *J–V* characteristics of thin film CdTe solar cells.

Table 1
Cell data for CdS/CdTe and type 1 and 2 $Cd_{1-x}Zn_xS$/CdS/CdTe solar cells

Cell type	V_{oc} (mV)	J_{sc} (mA/cm^2)	R_s (Ω cm^2)	R_{sh} (Ω cm^2)	FF	η (%)
CdS/CdTe	804	21.3	4.5	2150	0.67	11.4
1	739	21.9	5.0	889	0.62	10.0
2	727	21.8	10.3	1054	0.54	8.6

higher than that of CdS/CdTe. This mismatch increases with increase in Zn content in $Cd_{1-x}Zn_xS$. The V_{oc} of 625 mV that was previously reported [11] for $Cd_{1-x}Zn_xS$/CdTe and 630 mV for ZnS/CdTe solar cells [10] suggested that the defects due to this lattice incompatibility have a direct impact on this parameter. This study gives direct evidence that the lattice mismatch is indeed the culprit. For, our type 2 cells with Zn about the interface, in amount probably lower than the previous case [10,11], the V_{oc} is 727 mV. Whereas, the V_{oc} of type 1 cell with low Zn content is
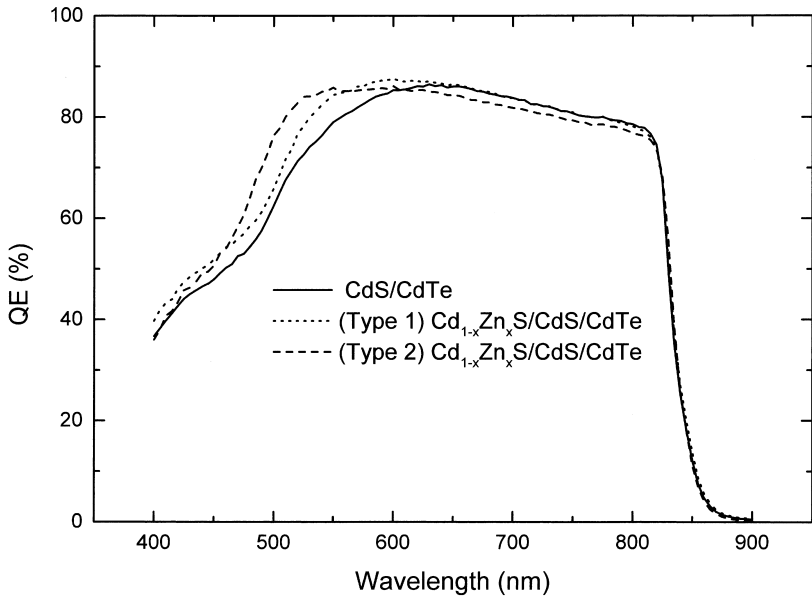
Fig. 4. Spectral response curves of CdTe thin film solar cells.

739 mV, and that CdS/CdTe cell with no Zn except those non-intentionally introduced in the structure during processing and the growth of the window layer from the CBD bath has 804 mV as its V_{oc}. Since it is the relative displacement of the quasi-Fermi energy levels at the interface that determines the solar cell V_{oc}, it is therefore logical to say that the lattice mismatch of the materials in this region does pin these levels restricting their motion, and hence the V_{oc} of the cell. The shunt resistance, the FF, and the efficiency are also affected by these defects as indicated by their values in the Table 1. Nevertheless, the 10% efficiency of our best $Cd_{1-x}Zn_xS/CdS/CdTe$ solar cell is much higher than [10] 2% of ZnS/CdTe and [11] 7% of $Cd_{1-x}Zn_xS/CdTe$ solar cells. Our design approach then represents the right approach if the present record [9] 16% efficiency of CdTe solar cell is to be raised further.

4. Conclusion

The thorough understanding of CBD growth mechanisms of ZnS and CdS and the improvement of their processing in the course of our previous studies [8] has enabled us to propose and fabricate a new CdTe solar cell structure.

The trend in the spectral response of our CdS/CdTe solar cell is same as that of CdS/CdTe that has produced 16% efficiency, the highest ever recorded [9] in CdTe solar cells. The 11.4% efficiency recorded in this study has to do with low quality soda lime glass. This glass has 3 mm thickness translating into low transmission. Plus, its absorption edge starts around 500 nm where AM1.5 is quite rich [3] in photons. It
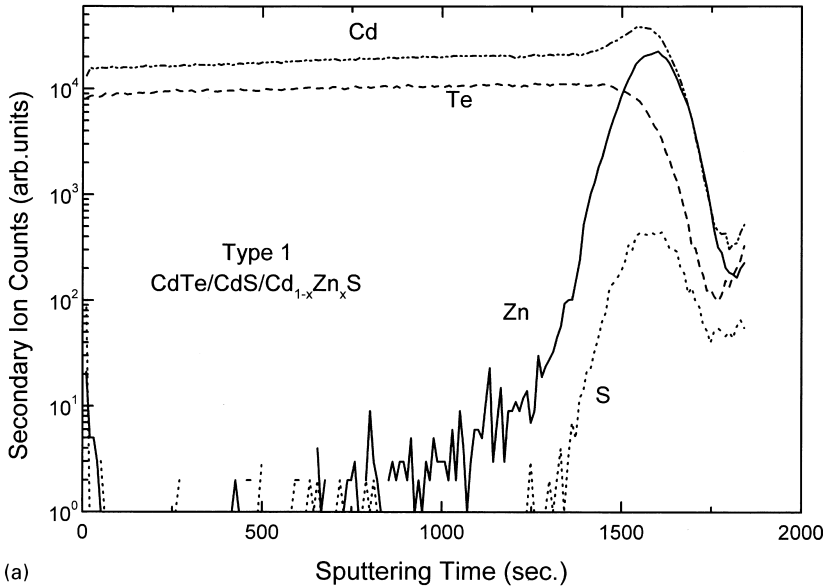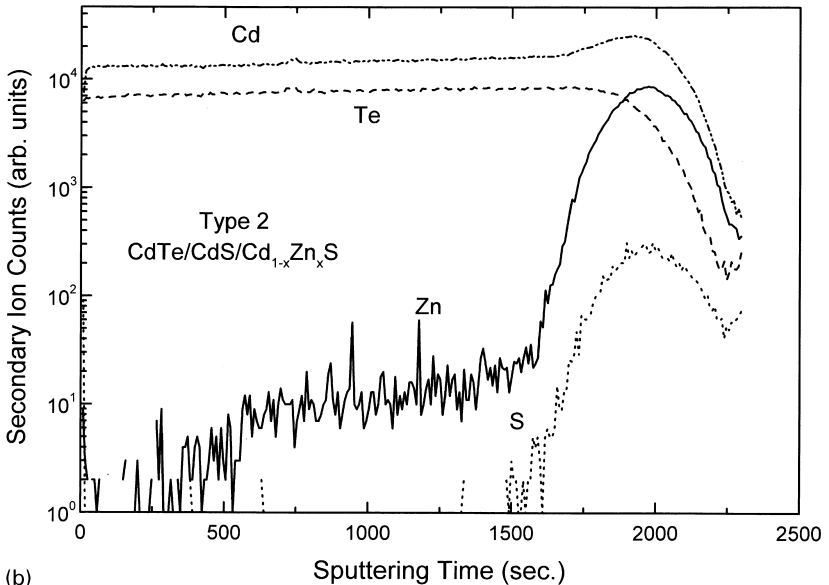
Fig. 5. SIMS depth profiles of (a) type 1 and (b) type 2 CSS-CdTe/CBD-CdS/$Cd_{1-x}Zn_xS$ solar cells.

also contains sodium that has the tendency of diffusing into the active film layers where they create defects or defect complexes that act as recombination centers. However, the spectral responses in the short wavelength region of AM1.5 of our $Cd_{1-x}Zn_xS$/CdS/CdTe solar cells are better than CdS/CdTe cells. Thus if the

thickness of $Cd_{1-x}Zn_xS$ and CdS films and the post-growth treatment can be optimized to minimize the Zn diffusion to the interface with a borosilicate glass used as the substrate, a record efficiency could be achieved. Nevertheless, in this study, using soda lime glass as the substrate with no anti-reflection coating we have produce a 10% efficient $Cd_{1-x}Zn_xS$ layer containing CdTe solar cell, the highest ever reported for this type of cell.

Acknowledgements

References

[1] H.J. Moller, Semiconductor for Solar Cells, Artech House, Boston, 1993.
[2] B. Ray, II–VI Compounds, Pergamon Press, Oxford, 1969.
[3] C. Ferekides, J. Britt, Y. Ma, L. Killiam, Proceedings of the Twenty Third IEEE photovoltaic Specialists Conference, 1993, p. 389.
[4] P. Capper, in: P. Capper (Ed.), Narrow-gap II–VI Compounds for Optoelectronic and Electromagnetic Applications, Chapman and Hall, New York, 1997, p. 211.
[5] K.L. Chopra, S.R. Das, Thin Film Solar Cell, Plenum Press, New York, 1983.
[6] W. Lehmann, in: S. Shinoya, H. Kobayashi (Eds.), Proceedings of the Fourth International Workshop on Electroluminescence, Vol. 38, Springer-Verlag, Berlin, 1989, p. 371.
[7] J.J. Liou, Advanced Semiconductor Device Physics and Modelling, Artech House, Boston, 1994, p. 105.
[8] I.O. Oladeji, Ph.D. Dissertation, University of Central Florida, 1999.
[9] H. Ohyama, T. Aramoto, S. Kumazawa, H. Higuchi, T. Arita, S. Shibutani, T. Nishio, J. Nakajima, M. Tsuji, A. Hanafusa, T. Hibino, K. Omura, M. Murozono, Proceedings of the Twenty sixth IEEE photovoltaic Specialists Conference, 1997, p. 343.
[10] D. M. Oman, Ph.D. Dissertation, University of South Florida, 1995.
[11] T.L. Chu, S.S. Chu, J. Britt, C. Ferekides, C.Q. Wu, Proceedings of the Twenty Second IEEE photovoltaic Specialists Conference, 1991, p. 1136.